*Metrol. Meas. Syst.*, Vol. 29 (2022), No. 1
DOI: 10.24425/mms.2022.138541

METROLOGY AND MEASUREMENT SYSTEMS

Index 330930, ISSN 0860-8229

*www.metrology.wat.edu.pl*

# DIAGNOSIS OF MULTIPLE FAULTS OF AN INDUCTION MOTOR BASED ON HILBERT ENVELOPE ANALYSIS

**Ahmet Kabul[1], Abdurrahman Ünsal[2]**

1) *Burdur Mehmet Akif Ersoy University, Department of Electrical and Electronics Engineering, 15030, Burdur, Turkey* (✉ *ahmetkabul@mehmetakif.edu.tr*, +90 248 213 2761).
2) *Kütahya Dumlupınar University, Department of Electrical and Electronics Engineering, 43100, Kütahya, Turkey* (*unsal@dpu.edu.tr*)

**Abstract**

Three phase induction motors are widely used in industrial processes therefore condition monitoring of these motors is important. Broken rotor bars, eccentricity and bearing faults are the most common types of faults of induction motors. Stator current and/or vibration signals are mostly preferred for the monitoring and detection of these faults. Fast Fourier Transform (FFT) based detection methods analyse the characteristic harmonic components of stator current and vibration signals for feature extraction. Several types of simultaneous faults of induction motors may produce characteristic harmonic components at the same frequency (with varying amplitudes). Therefore, the detection of multiple faults is more difficult than the detection of single fault by FFT based diagnosis methods. This paper proposes an alternative approach for the detection of simultaneous multiple faults including broken rotor bars, static eccentricity and outer-race or inner-race bearing faults by analysing stator current and vibration signals. The proposed method uses Hilbert envelope analysis with a Normalized Least Mean Square (NLSM) adaptive filter. The results are verified experimentally under 25%, 50%, 75%, 100% loading conditions.

Keywords: Hilbert envelope analysis, induction motor, multiple faults.



## 1. Introduction

Induction motors are widely preferred in industrial applications such as fans, conveyors, pumps, etc. due to their lower cost, easy maintenance and higher reliability. Induction motors may fail due to thermal stress, vibrations, mechanical forces and alignment problems. These multiple problems may occur simultaneously or consecutively [1, 2].

The distribution of induction motor faults is approximately presented as 69% bearing, 21% stator winding, 7% rotor faults and 3% as shaft/coupling and other faults [3]. Although the bearing faults have the highest percentage among motor faults, broken rotor bars and eccentricity faults may eventually result in bearing faults. Therefore, it is more important to detect the reason of bearing faults than detecting of bearing faults to reduce bearing damages.

Bearings are the most critical parts of induction motors [4]. Only 10% of bearings can reach their L10 life in industrial environment [5]. This may happen due to unqualified maintenance crew and insufficient knowledge, misalignment of motor-load, and simultaneous multiple faults [6]. In order to save bearings, it is important to properly monitor the whole spectrum of fault related characteristic harmonic components.

During the last decades, detection of single faults of three phase induction motors has been studied extensively. Few studies have been reported in diagnosis of multiple faults [7]. Several types of simultaneous faults (broken rotor bars, static eccentricity, and bearing faults) of induction motors may produce characteristic harmonic components at the same frequency (with


Article history: received April 27, 2021; revised July 31, 2021; accepted August 16, 2021; available online October 5, 2021.

varying amplitudes). Therefore, the detection of multiple faults is more difficult than the detection of single fault by *Fast Fourier Transform* (FFT) based methods.

Stator current signals, vibration signals, acoustic noise signals, temperature, induced voltage, air gap magnetic flux signals are the most commonly used signals for the diagnosing of faults of induction motors. FFT based methods are commonly used for the analysis of stator current and vibration signals [8]. Moreover, portable signal analysers also use FFT based methods to detect induction motor faults [9-11]. Although FFT is frequently used for the analysis of signals, it has some drawbacks. When the motor load is low, the frequencies of characteristic harmonic components of current signals due to broken rotor bars are very close to the frequency of fundamental component with low amplitudes (and mostly overshadowed by fundamental components) [12]. Therefore, FFT based methods are ineffective to detect to characteristic harmonic components by using stator current and vibration signals at lower motor loads [2, 13]. In addition, FFT based methods are limited at the analysis of non-stationary signals [14]. Therefore, FFT based methods are used along with some other methods such as Wavelet [15], *Multiple Signal Classification* (MUSIC) [16], *Artificial Neural Network* (ANN) [17], and *Artificial Intelligence* (AI) methods [18]. A summary of FFT based methods is presented in Table 1 [19-26].

Table 1. A summary of FFT based methods for diagnosing induction motor faults.

| Reference | Year | Signal analysing method | Fault type(s) | Analysed data |
|---|---|---|---|---|
| [19] | 2019 | *Motor Current Signature Analysis* (MCSA) - FFT and MCSA – *Discrete Wavelet Transform* (DWT) | Rolling element bearings | Current |
| [20] | 2019 | FFT for feature extraction | Rolling element bearings | Current |
| [21] | 2019 | FFT and *Principle Component Analysis* (PCA) | Broken end-ring and broken rotor bars | Current |
| [22] | 2018 | FFT, *Hilbert time – time* (HTT) and PCA | Rolling element bearings | Vibration |
| [23] | 2017 | FFT and wavelet de-noising | Rolling element bearings | Vibration |
| [24] | 2017 | FFT | Broken rotor bars and inner race bearing | Vibration |
| [25] | 2016 | FFT | Rolling element bearings | Vibration |
| [26] | 2016 | FFT – *Independent Component Analysis* (ICA) | Broken rotor bars and bearings | Current |

In this paper, an alternative method is proposed to detect simultaneous multiple faults of induction motors by using Hilbert envelope analysis along with a *Normalized Least Mean Square* (NLMS) adaptive filter. Both stator current and vibration signals are analysed by the proposed method.

The studied simultaneous faults are as follows:

Case 1: Static eccentricity, three-broken rotor bars and outer-race bearing faults

Case 2: Static eccentricity, three-broken rotor bars and inner-race bearing faults

This paper is organized as follows. Section 2 and 3 briefly present adaptive filter and Hilbert envelope analysis consecutively. The experimental test-bed and the implementation are presented in Section 4 and 5 respectively. The experimental results of the proposed method are given in Section 6. The paper is concluded with Section 7.

## 2. NLMS adaptive filter

The proposed method contains an NLMS adaptive filter to increase the accuracy of proposed method. The NLMS adaptive filter is used to eliminate noise in the current and vibration signals. The optimization of NLMS filter tap weights is given in (1).

$$w(n+1) = w(n) + \mu(n)e(n) + x(n) \tag{1}$$

where $e(n)$ is the error signal [27] (see Fig.1) Adaptive filter weight coefficients filter are updated by the step size factor $(\mu_n)$ at each iteration to minimize the error. The design of filter is implemented in MATLAB. The optimum filter order and the step size are chosen as 64 and 0.2 respectively to provide an acceptable accuracy and convergence time. The structure of adaptive filter is shown in Fig. 1.

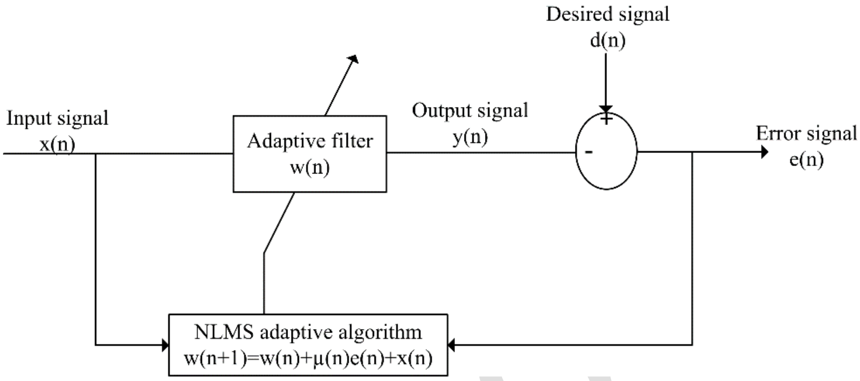

Fig. 1. General structure of the adaptive filter.

## 3. Hilbert envelope analysis

Envelope analysis is commonly used as a signal processing technique. The general process of Hilbert envelope analysis has four steps. First step is band pass filtering of stator current or vibration signals to focus on the frequencies of characteristic harmonic components. The second step is Hilbert transform. Hilbert transform is widely used to detect the faults of induction motors [2, 22, 28]. Suppose that $x(t)$ is a real time signal, Hilbert transform of $x(t)$ is given as follows (2)

$$H\{x(t)\} = \frac{1}{\pi t} * x(t) \tag{2}$$

The analytical signal $(z(t))$ can be written as in (3).

$$z(t) = x(t) + jh(t) \tag{3}$$

In third step is envelope analysis. The aim of this step is to square filtered time domain signal. The envelope of $z(t)$ can be calculated as given in (4)

$$E(t) = \sqrt{x^2(t) + h^2(t)} \tag{4}$$

In last step, the envelope spectrum is observed by performing the spectrum analysis to detect the fault related harmonic components.

## 4. The experimental test-bed

To verify the performance of the proposed method, an experimental test-bed was used. As shown in Fig. 2 the test-bed consists of a 3 $kW$ induction motor, a 5 $kVA$ self-excited synchronous generator, and a 5 $kW$ resistive load. The nameplate of the induction motor under test is shown in Table 2.

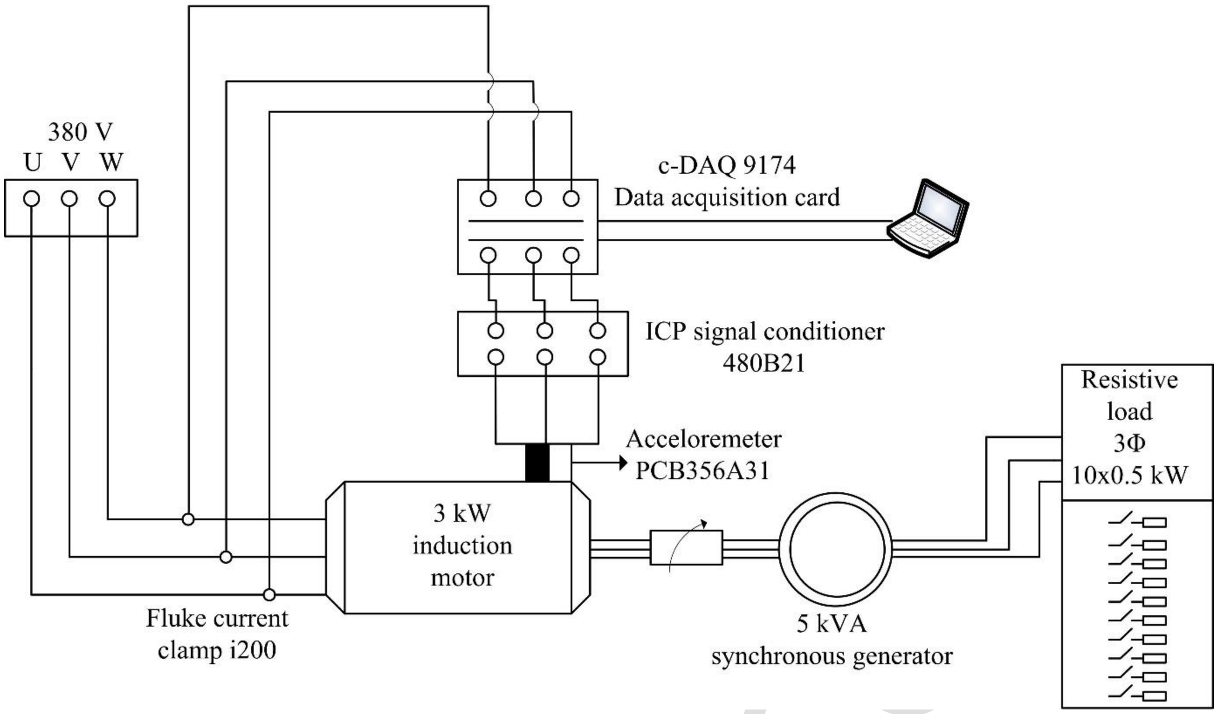


Fig. 2. The experimental test-bed.

Table 2. The nameplate rating of induction motor.

| Phase number | Connection type | Frequency (Hz) | Voltage (V) | Current (A) | Power (W) | Power factor | Speed (rpm) |
|---|---|---|---|---|---|---|---|
| 3 | Y | 50 | 380 | 5.9 | 3000 | 0.87 | 2850 |

Two types of fault scenarios (Case 1 and Case 2), were studied by the current and vibration signals under $25\%, 50\%, 75\%$ and $100\%$ loading levels of induction motor. To create static eccentricity fault, the bearing housing (Fig. 3(a)) of the end shield was expanded. A PLA (Polylactic Acid) based bushing, which was produced by a 3D printer (with static eccentricity), was placed into the bearing housing. Broken rotor bars were implemented by drilling three holes to the rotor bars (Please see Fig. 3(b)). 6206.C3 type bearing are used in the induction motor under test. The outer and inner race bearing faults were created by drilling holes on the outer and inner races of bearings respectively as shown in Fig. 3(c) and Fig. 3(d).

(a) (b) (c) (d)

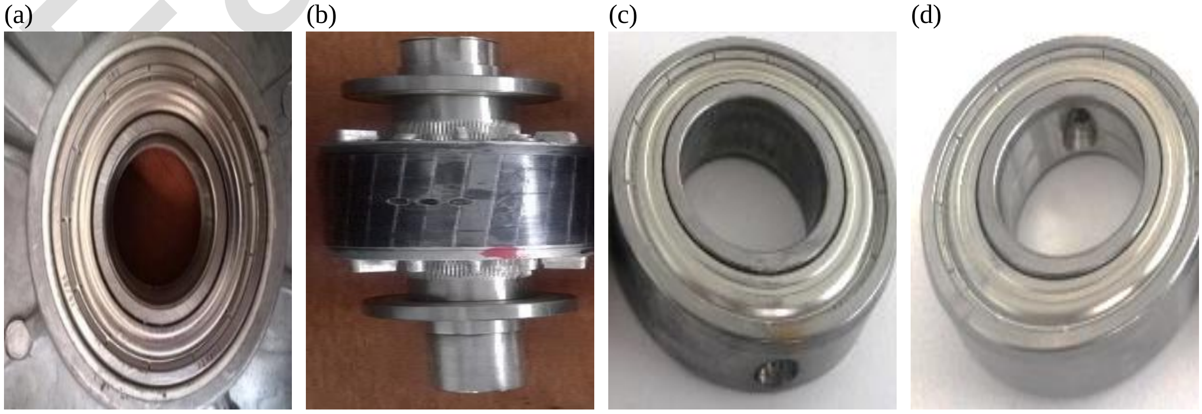

Fig. 3. Induction motor faults: static eccentricity fault (a), broken rotor bars (b), outer-race bearing faults (c), inner-race bearing faults (d).

## 5. Implementation

Both stator current and vibration signals were recorded with a sampling frequency of 25 $kHz$ by National Instrument NI c-DAQ 9174 data acquisition system (see Table 3). The analyses of the recorded signals were implemented in MATLAB environment. The noise signals are eliminated by the NLMS adaptive filter. Then Hilbert envelope analysis is applied to the filtered signal to detect harmonic components of current or vibration signals. The flowchart of the proposed method is presented in Fig. 4.

Table 3. The specifications of measurement devices.

| Type of signals | Measurement device | Amplifier | Data acquisition |
|---|---|---|---|
| Stator current | Fluke i200 AC current clamp | - | National instrument (NI) c-DAQ-9174 with NI 9225 module |
| Vibration | PCB three axis 356A31 model | 3 channel ICP sensor signal conditioner 480B21 model | National instrument (NI) c-DAQ-9174 with NI 9225 module |

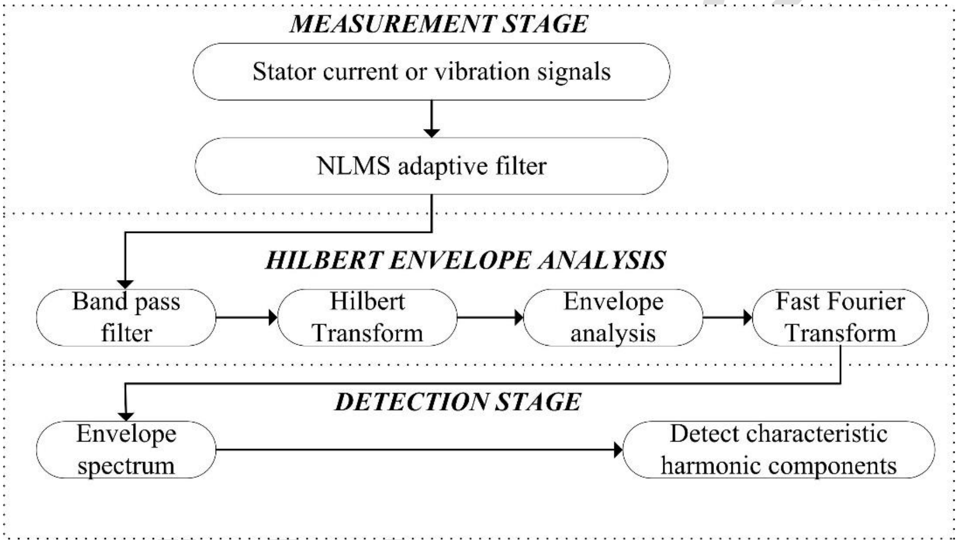


Fig. 4. Flowchart of the proposed method.

## 6. Results and discussion

A three phase, 3 $kW$ induction motor was used in this study. Two fault cases were studied. At case 1, static eccentricity, broken rotor bars and outer-race bearing faults were implemented simultaneously. At case 2, static eccentricity, broken rotor bars and inner-race bearing faults were implemented. At each test case both stator current and vibration signals were recorded.

### *6.1. Case 1: Static eccentricity, broken rotor bars and outer-race bearing faults*

#### *6.1.1. The analysis of stator current signals (Case 1)*

The frequencies of the static eccentricity characteristic harmonic components ($f_{ecn}$) can be calculated by using (5) [29].

$$f_{ecn} = f_s \pm k f_r \tag{5}$$

where $f_s$ is the fundamental component of supply frequency, $k = 1, 2, 3$ and $f_r$ is the rotor (shaft) frequency.

The frequencies of broken rotor bars characteristic harmonic components ($f_{brb}$) as follows (6) [12]

$$f_{brb} = (1 \pm 2ks) * f_s \quad (6)$$

where $s$ is the slip. In envelope spectrum, the characteristic harmonic component of broken rotor bars is calculated by employing $f_s - f_{brb}$ [30].

The frequencies of bearing faults characteristic harmonic components in the stator current signals are calculated by using (7) [31]

$$f_{bear} = |f_s \pm k * BPFO| \quad (7)$$

where $k = 2, 3, 4$ for visible corresponding harmonic components in current spectra. In (7), BPFO is defined as "Ball Pass Frequency Outer" or "Outer-Race Failing Frequency".

The frequency of the outer-race bearing fault characteristic harmonic components is calculated by using (8) [31].

$$BPFO = \frac{N_b}{2} * f_r * \left(1 - \frac{B_d}{P_d} * \cos\varphi\right) \quad (8)$$

where $N_b$ is the number of balls, $B_d$ is the ball diameter and $P_d$ is the pitch diameter, and $\varphi$ is the ball contact angle. The specifications of the bearing are given in Table 4.

Table 4. Data sheet of 6206 bearing [32].

| **Bearing number** | $N_b$ **(Qty)** | $B_d$ **(mm)** | $P_d$ **(mm)** | $\varphi$ **(°)** |
|---|---|---|---|---|
| 6206 | 9 | 9.525 | 46 | 0 |

The frequency of the outer-race bearing fault characteristic harmonic components is calculated by using the specifications of 6206 bearing as presented in (9).

$$BPFO = \frac{9}{2} * f_r * \left(1 - \frac{9.525}{46} * \cos 0\right) = 3.58 * f_r \quad (9)$$

The corresponding characteristic harmonic components of current spectra of outer-race bearing faults are presented in Table 5 based on (7).

Table 5. Current spectra of characteristic harmonic components of outer-race bearing faults.

| **Loading level (%)** | **Ball pass frequency of outer-race (Hz)** | **2nd current spectra harmonic (Hz)** | **3rd current spectra harmonic (Hz)** | **4th current spectra harmonic (Hz)** |
|---|---|---|---|---|
| 25 | 177.2 | 304 | 482 | 659 |
| 50 | 175.0 | 300 | 475 | 650 |
| 75 | 172.9 | 296 | 469 | 642 |
| 100 | 170.6 | 291 | 462 | 632 |

The results of the proposed method applied to the current signals for fault case 1 are shown in Table 6 and Fig. 5.

Table 6. The frequencies of characteristic harmonic components of current analysis for fault case 1.

| **Loading level (%)** | $f_r$ **(Hz)** | **Broken rotor bars harmonic frequency (Hz)** | **1st harmonic component of static eccentricity (Hz)** | **Outer-race bearing fault 2nd harmonic component (Hz)** |
|---|---|---|---|---|
| 25 | 49.5 | 0.954 | 99.50 | 304 |
| 50 | 48.9 | 2.193 | 98.95 | 300 |
| 75 | 48.3 | 3.386 | 98.56 | 296 |
| 100 | 47.7 | 4.721 | 97.22 | 291 |

DOI: 10.24425/mms.2022.138541

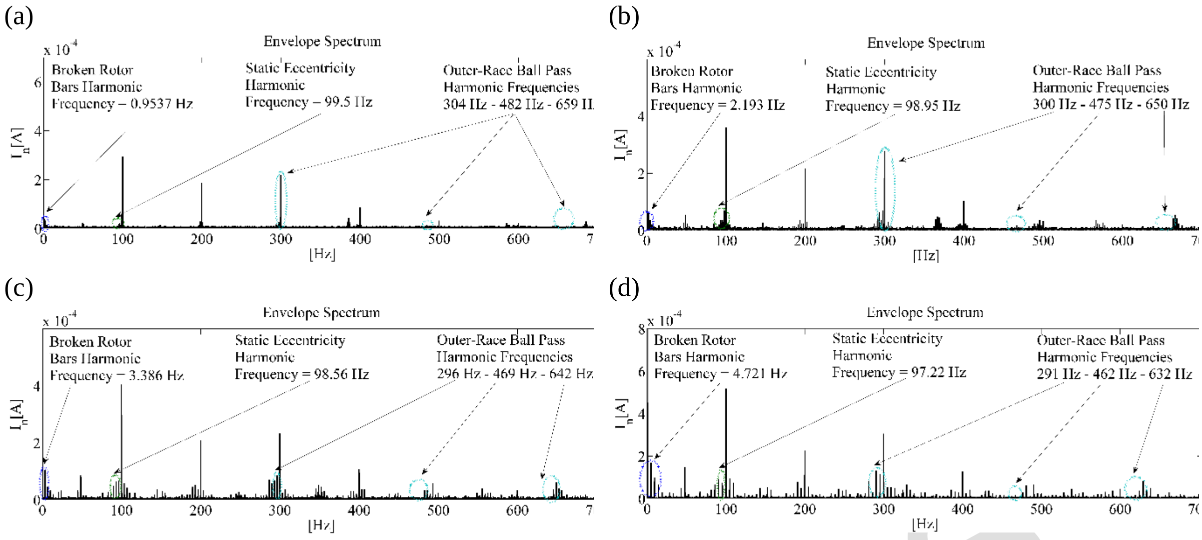


Fig. 5. Characteristic harmonic components of current signal under 25% loading (a), 50% loading (b), 75% loading (c), 100% loading (d) level of induction motor.

$I_n$ represents the amplitudes of normalized stator current signals in all figures. In FFT method, the characteristic harmonic components are detected in pairs as side-bands of the fundamental component. By using the proposed method, the characteristic harmonic components are detected without observing fundamental component when multiple faults are present. The low-amplitude characteristic harmonic components of broken rotor bars are shifted to $0 - 10$ Hz in envelope spectrum. Therefore, the proposed method offers an effective solution for overshadowing problems of dominant harmonic components as presented in Fig. 6. Moreover, the characteristic harmonic components of static eccentricity and outer-race bearing faults are detected successfully by the proposed method.

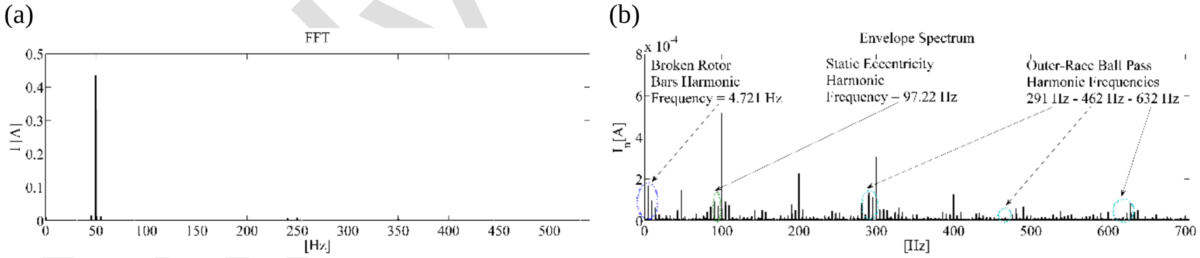


Fig. 6. FFT (a) and Hilbert envelope analysis (b) for the analysis of stator current signals at 100% loading level of induction motor.

### *6.1.2. The analysis of vibration signals (Case 1)*

The static eccentricity faults of the induction motor are detected by comparing the amplitudes of $kf_r$ characteristic harmonic components [33]. If the amplitude of $2f_r$ is greater or equal to 1.5 time with the amplitude of $f_r$, the static eccentricity fault is present.

The frequencies of the characteristic harmonic components of broken rotor bars ($f_{brb}$) are calculated as in (10) [34].

$$f_{brb} = f_r \pm 2ksf_s \tag{10}$$

Hilbert envelope analysis focuses on the $2ksf_s$ harmonic components.

The frequency of characteristic harmonic components of outer-race bearing fault is calculated as presented in (11).

$$BPFO = \frac{9}{2} * f_r * \left(1 - \frac{9.525}{46} * \cos 0\right) = 3.58 * f_r \tag{11}$$

The results of the proposed method applied to the vibration signals for fault case 1 are presented in Table 7 and Fig. 7.

Table 7. The frequencies of characteristic harmonic components of vibration analysis for fault case 1.

| **Loading level (%)** | $f_r$ **(Hz)** | $\frac{\text{Amplitude}(2f_r)}{\text{Amplitude}(f_r)}$ | **Ball pass harmonic frequency of outer-race (Hz)** | **Broken rotor bars harmonic frequency (Hz)** |
|---|---|---|---|---|
| 25 | 49.5 | 1.98 | 177.2 | 0.954 |
| 50 | 48.9 | 1.54 | 175.0 | 2.098 |
| 75 | 48.3 | 1.52 | 172.9 | 3.580 |
| 100 | 47.7 | 1.71 | 170.6 | 4.864 |

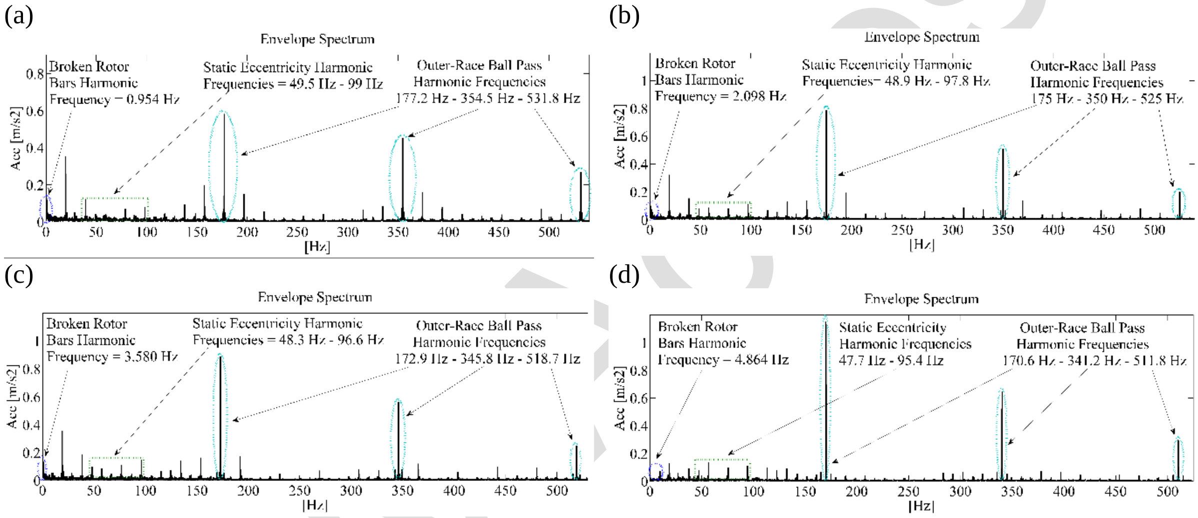


Fig. 7. Characteristic harmonic components of vibration signal under 25% loading (a), 50% loading (b), 75% loading (c), 100% loading (d) level of induction motor.

Figure 8 shows that the proposed method is capable of detecting fault harmonics as FFT method at 100% loading condition in vibration analysis. The characteristic harmonic components of static eccentricity and outer-race bearing faults are detected successfully (with greater amplitudes) when they are compared to the results of FFT. Since, the harmonic components of broken rotor bars are shifted to $0 - 10$ Hz frequency region, the proposed method offers an effective solution for overshadowing problems of dominant harmonic components as presented in Fig. 8.

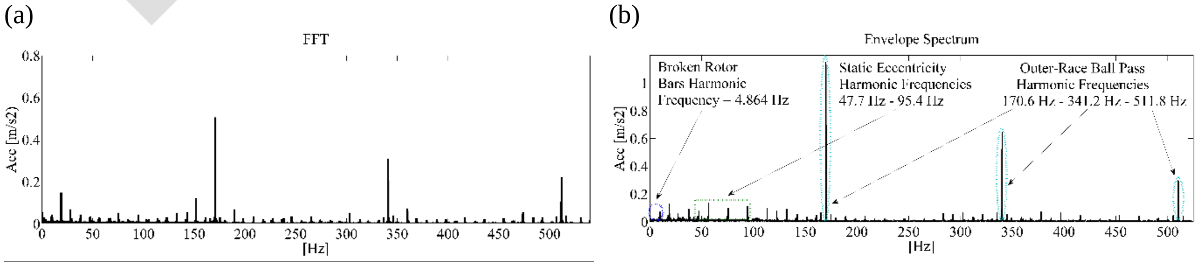


Fig. 8. FFT (a) and Hilbert envelope analysis (b) for the analysis of vibration signals at 100% loading level of induction motor.

### *6.2. Case 2: Static eccentricity, broken rotor bars and inner race bearing faults*

#### *6.2.1. The analysis of stator current signals (Case 2)*

The frequencies of bearing fault characteristic harmonic components by employing stator current signals are calculated as given in (12) [31].

$$f_{bear} = |f_s \pm k * BPFI| \tag{12}$$

where $k = 2, 3, 4$ for visible corresponding harmonic components in current spectra. In (12), BPFI is defined as "Ball Pass Frequency Inner" or "Inner-Race Failing Frequency".

The frequency of the inner-race bearing fault characteristic harmonic components is calculated by using (13) [31].

$$BPFI = \frac{N_b}{2} * f_r * \left(1 + \frac{B_d}{P_d} * \cos\varphi\right) \tag{13}$$

The frequency of the inner-race bearing fault characteristic harmonic components is calculated by using the specifications of 6206 bearing as presented in (9)

$$BPFI = \frac{9}{2} * f_r * \left(1 + \frac{9.525}{46} * \cos 0\right) = 5.43 * f_r \tag{14}$$

The corresponding frequencies of characteristic harmonic components of inner-race bearing faults are presented in Table 8 based on (12).

Table 8. Current spectra of characteristic harmonic components of inner-race bearing faults.

| **Loading level (%)** | **Ball pass frequency of inner-race (Hz)** | **2nd current spectra harmonic (Hz)** | **3rd current spectra harmonic (Hz)** | **4th current spectra harmonic (Hz)** |
|---|---|---|---|---|
| 25 | 267.4 | 585 | 852 | 1120 |
| 50 | 263.6 | 577 | 841 | 1104 |
| 75 | 260.3 | 571 | 831 | 1091 |
| 100 | 256.6 | 563 | 820 | 1076 |

The results of the proposed method applied to the current signals for the fault case 2 are given in Table 9 and Fig. 9.

Table 9. The frequencies of characteristic harmonic components of current analysis for fault case 2.

| **Loading level (%)** | $f_r$ **(Hz)** | **Broken rotor bars harmonic frequency (Hz)** | **1st harmonic component of static eccentricity (Hz)** | **Inner-race bearing fault 2nd harmonic component (Hz)** |
|---|---|---|---|---|
| 25 | 49.2 | 0.954 | 99.2 | 585 |
| 50 | 48.6 | 2.200 | 98.6 | 577 |
| 75 | 47.9 | 3.390 | 98.0 | 571 |
| 100 | 47.3 | 4.780 | 97.3 | 563 |

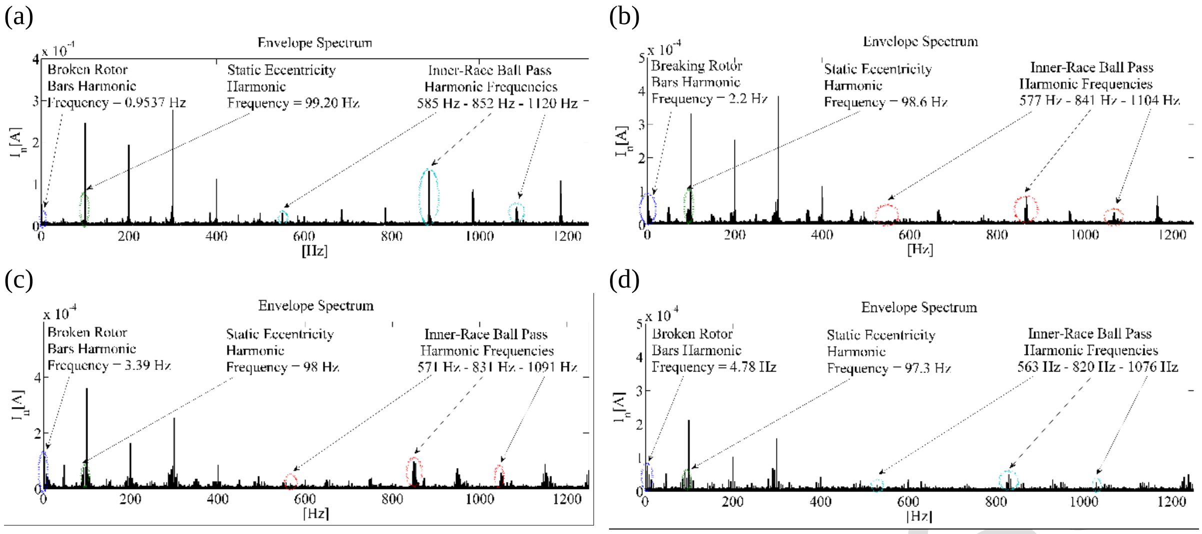


Fig. 9. Characteristic harmonic components of current signal under 25% loading (a), 50% loading (b), 75% loading (c), 100% loading (d) level of induction motor.

Figure 10 presents the effectiveness of the proposed method as it is compared to FFT to detect fault related harmonic components at 100% loading conditions.

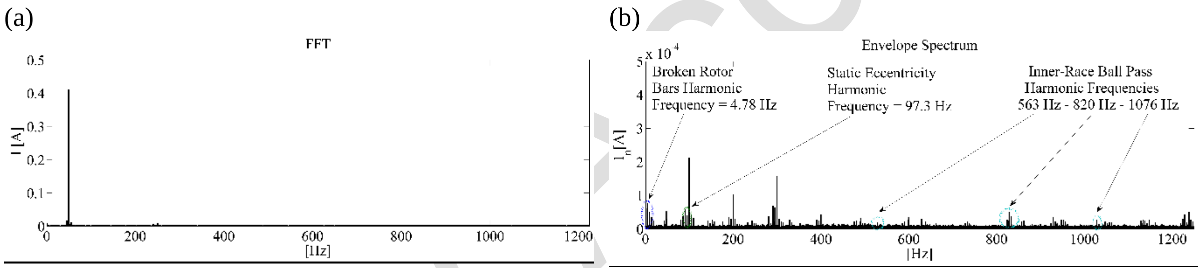


Fig. 10. Comparing of FFT (a) and Hilbert envelope analysis (b) for the analysis of current signals at 100% loading level of induction motor.

### *6.2.2. The analysis of vibration signals (Case 2)*

The frequency of the characteristic harmonic components of inner-race bearing fault is calculated as in (15).

$$BPFI = \frac{9}{2} * f_r * \left(1 + \frac{9.525}{46} * \cos 0\right) = 5.43 * f_r \qquad (15)$$

The results of the proposed method applied to the vibration signals for the fault case 2 are shown in Table 10 and Fig. 11.

Table 10. The frequencies of characteristic harmonic components of vibration analysis for fault case 2.

| **Loading level (%)** | $f_r$ **(Hz)** | $\frac{\mathbf{Amplitude(2f_r)}}{\mathbf{Amplitude(f_r)}}$ | **Ball pass harmonic frequency of inner-race (Hz)** | **Broken rotor bars harmonic frequency (Hz)** |
|---|---|---|---|---|
| 25 | 49.5 | 2.52 | 267.4 | 1.001 |
| 50 | 48.6 | 2.09 | 263.6 | 2.289 |
| 75 | 48.0 | 1.71 | 260.3 | 3.529 |
| 100 | 47.3 | 2.27 | 256.6 | 4.721 |

DOI: 10.24425/mms.2022.138541

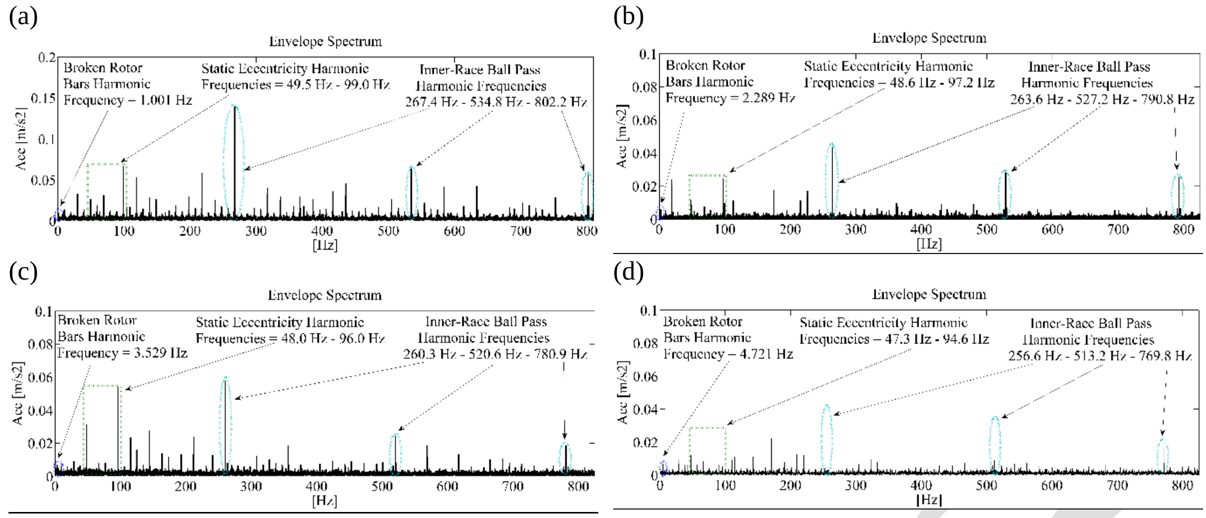


Fig. 11. Harmonic components of vibration signal under 25% loading (a), 50% loading (b), 75% loading (c), 100% loading (d) level of induction motor.

Figure 12 shows that the proposed method is capable of detecting fault harmonics as FFT method at 100% loading condition in vibration analysis.

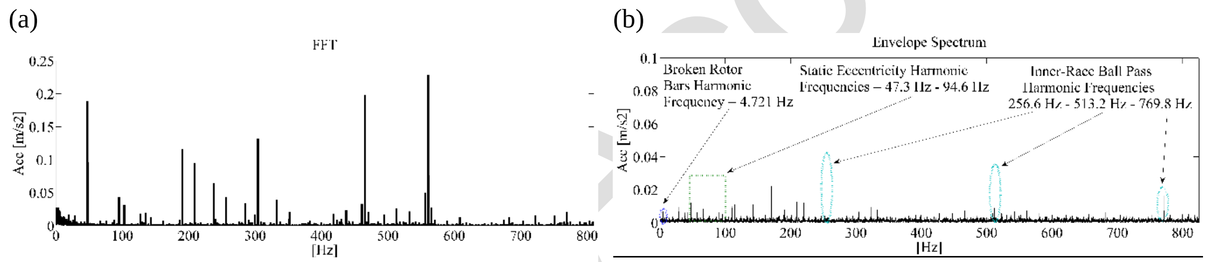


Fig. 12. FFT (a) and Hilbert envelope analysis (b) for the analysis of vibration signals at 100% loading level of induction motor.

## 7. Conclusions

In this paper, simultaneous multiple faults including static eccentricity, broken rotor bars, outer or inner race bearing faults of a 3 $kW$ induction motor under 25%, 50%, 75% and 100% loading levels are investigated by applying Hilbert envelope analysis to the stator current and vibration signals.

The FFT based methods are limited when the motor is lightly loaded with simultaneous faults. The performance of the proposed method has been tested under varying loading levels of induction motor. The results show that the performance of the proposed method is better than the performance of FFT analysis of the current signals of induction motor with simultaneous faults at low loading levels. It can be seen in Fig. 6 (case 1) and Fig 10 (case 2), the low amplitudes of characteristic harmonic components would not be properly detected by the FFT method (even if the induction motor operates at full load) due to the existence of dominant fundamental component of characteristic harmonic components.

Although FFT method offers superior results in the detection of characteristic harmonic components of static eccentricity and bearing faults based on vibration signals, it is limited in the detection of broken rotor bars. The results show that the proposed method successfully detects the characteristic harmonic components of simultaneous broken rotor bars, static eccentricity and outer-race or inner-race bearing faults at four different loading levels of induction motor by using vibration signals. In addition, the proposed method solves the overshadowing problems of characteristic harmonic components of broken rotor bars and static eccentricity faults of induction motor at low loading levels by dominant fundamental component.

The major contribution of this work is the successful detection of low amplitude characteristic harmonic components of simultaneous faults of induction motors.

## Acknowledgements

This study was supported by The Scientific and Technological Research Council of Turkey (TUBITAK) with a grant number of 116E302.

## References

[1] Tousizadeh, M., Che, H. S., Selvaraj, J., Rahim, N. A., & Ooi, B.-T. (2019). Fault-tolerant field-oriented control of three-phase induction motor based on unified feedforward method. *IEEE Transactions on Power Electronics*, *34*(8), 7172-7183. https://www.doi.org/10.1109/TPEL.2018.2884759

[2] Matic, D. & Kanovic, Z. (2017). Vibration based broken bar detection in induction machine for low load conditions. *Advances and Electrical and Computer Engineering*, *17*(1), 49-54. https://www.doi.org/10.4316/AECE.2017.01007

[3] Liang, X., Ali, M. Z., & Zhang, H. (2020). Induction motors fault diagnosis using finite element method: A review. *IEEE Transactions on Industry Applications*, *56*(2), 1205-1217. https://www.doi.org/10.1109/TIA.2019.2958908

[4] Jiang, Q., Chang, F. & Sheng, B. (2019). Bearing fault classification based on convolutional neural network in noise environment. *IEEE Access*, *7*, 69795-69807. https://www.doi.org/10.1109/ACCESS.2019.2919126

[5] Peeters, C., Guillaume, P. & Helsen, J. (2018). Vibration-based bearing fault detection for operations and maintenance cost reduction in wind energy. *Renewable Energy*, *116*, 74-87. https://www.doi.org/10.1016/j.renene.2017.01.056

[6] Ünsal, A. (2020). Investigation of parallel misalignment faults of induction motor by using entropy analysis. *Journal of Polytechnic*, *23*(4), 1037-1050. https://www.doi.org/10.2339/politeknik.551490

[7] Saucedo-Dorantes, J. J., Delgado-Prieto, M., Ortega-Redondo, J. A., Osornio-Rios, R. A. & Romero-Troncoso, R. d. J. (2016). Multiple-fault detection methodology based on vibration and current analysis applied to bearings in induction motors and gearboxes on the kinematic chain. *Shock and Vibration*, *2016*, 1-13. https://www.doi.org/10.1155/2016/5467643

[8] Toliyat, H. A., Nandi, S., Choi, S. & Meshgin-Kelk, H. (2013). *Electric machines, modeling, condition monitoring, and fault diagnosis* (p. 99). CRC Press.

[9] NPP KOHTECT. (29.04.2021). *Vibration Analyzer Data Collector 107VF*. http://www.koh-tect.com/data/products/413822819605767497f351.pdf

[10] RECOVIB®. (29.04.2021). *RECOVIB FEEL 3-Axis Shock & Vibration Smart Probe*. https://micromega-dynamics.com/wp-content/uploads/2020/01/Recovib_FEEL_EN-Rev1p0.pdf

[11] ERBESSD INSTRUMENT®. (29.04.2021). *DigivebeMX® Vibration Analyzer, Data Collector&Dynammic Balancer*. https://www.spectran.co.za/attachments/DigivibeMX-FINAL_sAs.pdf

[12] Günal, S., Ece D. G. & Gerek Ö. N. (2009). Induction machine condition monitoring using notch-filtered motor current. *Mechanical Systems and Signal Processing*, *23*, 2658-2670. https://www.doi.org/10.1016/j.ymssp.2009.05.011

[13] Unsal, A. & Kabul, A. (2016). Detection of the broken rotor bars of squirrel-cage induction motors based on normalized least mean square filter and Hilbert envelope analysis. Electrical Engineering, *98*(3), 245-256. https://doi.org/10.1007/s00202-016-0366-5

[14] Romero-Troncoso, R. d. J. (2016). Multirate signal processing to improve FFT-based analysis for detecting faults in induction motors. *IEEE Transactions on Industrial Informatics*, *13*(3), 1291-1300. https://www.doi.org/10.1109/TII.2016.2603968

[15] Liu, M. & Weng, P. Y. (2019). Fault diagnosis of ball bearing elements: A generic procedure based on time-frequency analysis. *Measurement Science Review, 19*(4), 185-194. https://www.doi.org/10.2478/msr-2019-0024

[16] Elbouchikhi, E., Choqueuse, V. & Benbouzid, M. (2016). Induction machine bearing faults detection based on a multi-dimensional MUSIC algorithm and maximum likelihood estimation. *ISA Transactions, 63*, 413-424. https://www.doi.org/10.1016/j.isatra.2016.03.007

[17] Chen, Z., Deng, S., Chen, X., Sanchez, R.-V. & Quin, H. (2017). Deep neural networks-based rolling bearing fault diagnosis. *Microelectronics Reliability, 75*, 327-333. https://www.doi.org/10.1016/j.microrel.2017.03.006

[18] Unal, M., Onat, M., Demetgul, M. & Kucuk, H. (2014). Fault diagnosis of rolling bearings using a genetic algorithm optimized neural network. *Measurement, 58*, 187-196. https://www.doi.org/10.1016/j.measurement.2014.08.041

[19] Bessous, N., Sbaa, S. & Megherbi, A. C. (2019). Mechanical fault detection in rotating electrical machines using MCSA-FFT and MCSA-DWT techniques. *Bulletin of the Polish Academy of Sciences: Technical Sciences, Vol 67*(3), 571-582. https://www.doi.org/10.24425/bpasts.2019.129655

[20] Pandarakone, S. E., Mizuno Y. & Nakamura H. (2019). A comparative study between machine learning algorithm and artificial intelligence neural network in detecting minor bearing fault of induction motors. *Energies, 12*(11), 2105. https://doi.org/10.3390/en12112105

[21] Yoo Y. J. (2019). Fault detection of induction motor using Fast Fourier Transform with feature selection via Principal Component Analysis. *International Journal of Precision Engineering and Manufacturing, 20*, 1543-1552. https://www.doi.org/10.1007/s12541-019-00176-z

[22] Pang, B., Tang, G., Tian, T. & Zhou, C. (2018). Rolling bearing fault diagnosis based on improved HTT transform. *Sensors, 18*(4), 1203. https://www.doi.org/10.3390/s18041203

[23] Mishra, C., Samantaray, A. K. & Chakraborty, G. (2017). Rolling element bearing fault diagnosis under slow speed operation using wavelet de-noising. *Measurement, 103*, 77-86. https://www.doi.org/10.1016/j.measurement.2017.02.033

[24] Naha, A., Thammayyabbabu, K. R., Samanta, A. K., Routray, A. & Deb, A. K. (2017). Mobile application to detect induction motor faults. *IEEE Embedded Systems Letters, 9*(4), 117-120. https://www.doi.org/10.1109/LES.2017.2734798

[25] Maruthi, G. S. & Hegde, V. (2016). Application of MEMS accelerometer for detection and diagnosis of multiple faults in the roller element bearings of three phase induction motor. *IEEE Sensors Journal, 16*(1), 145-152. https://www.doi.org/10.1109/JSEN.2015.2476561

[26] Yang, T., Pen, H., Wang, Z. & Chang, C. S. (2016). Feature knowledge based fault detection of induction motors through the analysis of stator current data. *IEEE Transactions on Instrumentation and Measurement, 65*(3), 549-558. https://www.doi.org/10.1109/TIM.2015.2498978

[27] Yu, Z., Cai, Y. & Mo, D. (2020). Comparative study on noise reduction effect of fiber optic hydrophone based on LMS and NLMS algorithm. *Sensors, Vol 20*(1), 301. https://www.doi.org/10.3390/s20010301

[28] Kabul, A. & Ünsal, A. (2021). An alternative approach for the detection of broken rotor bars and bearing faults of induction motor based on vibration signals. *Proceedings of the 8th International Conference on Electrical and Electronics Engineering (ICEEE)*, Turkey, 126-131. https://www.doi.org/10.1109/ICEEE52452.2021.9415920

[29] Faiz, J. & Moosavi S. M. M. (2016). Eccentricity fault detection – Frominductionmachines toDFIG—A review. *Renewable and Sustainable Energy Reviews, 55*, 169-179. https://www.doi.org/10.1016/j.rser.2015.10.113

[30] Kabul, A. & Ünsal, A. (2021). Detection of broken rotor bars of induction motors based on the combination of Hilbert envelope analysis and Shannon entropy. *tm - Technisches Messen, 88*(1), 45-58. https://www.doi.org/10.1515/teme-2020-0066

[31] Boudinar, A. H., Benouzza, N., Bendiabdellah, A. & Khodja, M.-E.-A. (2016). Induction motor bearing fault analysis using a Root-MUSIC method. *IEEE Transactions on Industry Applications, Vol 52*(5), 3851-3860. https://www.doi.org/10.1109/TIA.2016.2581143

[32] GBMN Bearing USA Ltd. (29.04.2021). *Data Sheet of 6206 Bearing.* https://www.gmnbt.com/catalog/product/bb-6206-radial-ball-bearing/

[33] Hujare, D. P. & Karnik, M. G. (2018). Vibration responses of parallel misalignment in Al shaft rotor bearing system with rigid coupling. *Materials Today: Proceedings*, *5*(11), 23863-23871. https://www.doi.org/10.1016/j.matpr.2018.10.178

[34] Wang, Z., Yang, J., Li, H., Zhen, D., Xu Y. & Gu, F. (2019). Fault identification of broken rotor bars in induction motors using an improved cyclic modulation spectral analysis. *Energies*, *12*(17), 3279. https://www.doi.org/10.3390/en12173279

**Ahmet Kabul** received his B.S. in electrical-electronics engineering from Anadolu University, Eskisehir, Turkey, in 2009; his M.S. in electrical-electronics engineering from Dumlupinar University, Kutahya, Turkey, in 2013. He is currently pursuing the Ph.D. degree in electrical-electronics engineering with Kutahya Dumlupinar University. From 2009-2018, he worked as a research assistant in Dumlupinar University. From March 2018-May 2019, he worked in a textile factory as a maintenance engineer. From May 2019 to present, he has been with the Department of Electrical-Electronics Engineering of Burdur Mehmet Akif Ersoy University as a research assistant. His research interests include diagnosing of induction motor failures.

**Abdurrahman Ünsal** received his B.S. from Gazi University (Ankara/Turkey) in 1992, M.S. degree from Oklahoma State University (USA) in 1996, and Ph.D. degree from Oregon State University (USA) in 2001. He is currently working as a Professor at the Department of Electrical and Electronics Engineering of Kutahya Dumlupinar University in Turkey. His research interests are power quality, fault detection and control of electrical machines, renewable energy, and smart grids. He is an IEEE member since 2000.